A novel impedimetric glucose biosensor based on immobilized glucose oxidase on a CuO-Chitosan nanobiocomposite modified FTO electrode

Padideh Naderi Asrami, Sayed Ahmad Mozaffari, Mohammad Saber Tehrani, Parviz Aberoomand Azar

PII: S0141-8130(18)31758-6
DOI: doi:10.1016/j.ijbiomac.2018.05.228
Reference: BIOMAC 9833

To appear in: *International Journal of Biological Macromolecules*

Received date: 14 April 2018
Revised date: 30 May 2018
Accepted date: 30 May 2018

Please cite this article as: Padideh Naderi Asrami, Sayed Ahmad Mozaffari, Mohammad Saber Tehrani, Parviz Aberoomand Azar , A novel impedimetric glucose biosensor based on immobilized glucose oxidase on a CuO-Chitosan nanobiocomposite modified FTO electrode. Biomac (2017), doi:10.1016/j.ijbiomac.2018.05.228

A novel impedimetric glucose biosensor based on immobilized glucose oxidase on a CuO-Chitosan nanobiocomposite modified FTO electrode

Padideh Naderi Asrami [a], Sayed Ahmad Mozaffari [b,*], Mohammad Saber Tehrani [a], Parviz Aberoomand Azar [a]

[a] *Department of Chemistry, Science and Research Branch, Islamic Azad University, Tehran, Iran.*

[b] *Thin Layer and Nanotechnology Laboratory, Department of Chemical Technology, Iranian Research Organization for Science and Technology (IROST), P.O. Box 33535-111, Tehran. Iran.*

Corresponding author: E-mail: mozaffari@irost.ir

Tel: +98 21 56276637 Fax: +98 21 56276265

Abstract

This research aims at elaborating on the construction of a novel nanostructured copper oxide (Nano-CuO) sputtered thin film on the conductive fluorinated-tin oxide (FTO) layer that was exploited to immobilize glucose oxidase (GOx) enzyme via chitosan for developing impedimetric glucose biosensing. The distinct Nano-CuO thin film was fabricated by reactive DC magnetron sputtering system at the optimized instrumental deposition conditions. The FTO/Nano-CuO/Chitosan/GOx biosensor containing several layers afforded excellent microenvironment for rapid biocatalytic reaction to glucose. Field emission-scanning electron microscopy (FE-SEM), Ultraviolet–Visible spectroscopy (UV-Vis), cyclic voltammetry (CV), and electrochemical impedance spectroscopy (EIS) were established the morphology of modified electrode's surface and electrochemical behavior of glucose on the fabricated biosensor. Characterization of the surface morphology and roughness of CuO thin film by FE-SEM exhibits cavities of the nanoporous film as an effective biosensing area for covalent enzyme immobilization. Invented FTO/Nano-CuO/Chitosan/GOx biosensor was employed for glucose determination using the impedimetric technique. The impedimetric outcomes display high sensitivity for glucose (0.261 kΩ per mM) detection within 0.2–15 mM and limit of detection as 27 μM. The declared biosensor has been applied as a careful, noncomplicated, and exact biosensor for recognition of glucose in the real samples analysis.

Keywords: CuO-Chitosan nanobiocomposite; Glucose biosensor; Reactive DC magnetron sputtering.

1. Introduction

Recently, global statistical data shown that there are more than 422 million people in the world suffering from diabetes mellitus and the patient numbers keep growing. Although diabetes mellitus, a chronic disease, could be effectively treated and control, it is desired to further improve the performance of the apparatus for precisely monitoring patients' glucose levels which are actually more or less than the appropriate level of 4.4-6.6 mM [1-4]. Due to the fact that guaranteed and quick glucose level quantification is very crucial in different fields like food industry [5], clinical diagnostics, and biotechnology; the emergence of electrochemical glucose sensor has been focused on by many researchers [6-8].

Highly sensitive, reliable and disposable biosensors which can be used for recognizing glucose in urine and blood samples for the detection of diabetes are highly desired. Enzyme-based electrochemical biosensors are currently used in areas such as health care, food safety, and environmental monitoring. Glucose oxidase (GOx), which is used in glucose biosensors, was used as a model of an enzyme. It is important to note that glucose biosensors represent the largest market for biosensors. It has been reported that glucose biosensors dominate commercial biosensor products and account for approximately 85% of the entire world market for biosensors.

Nowadays several attempts have been widely done to develop glucose electrochemical biosensors, due to their inherent advantages such as robustness, easy miniaturization, excellent detection limits, and a requirement for very small amounts of analyte. Furthermore, electrochemical methods respond faster and remain stable for a longer time. Although the performance of an enzyme-based biosensor depends on the function of the transducer, the heart of a biosensor is the enzyme, which converts the substrate into the product(s), providing electronic signals to the transducer. The transducer then converts the electronic signals into an easily measurable signal, which can be displayed in the form of the desired units [9, 10]. Many procedures and methods are being proposed for producing new glucose biosensors, such as colorimetric [11], conductometric [12], optical [13, 14], and fluorescent spectroscopy [15] methods. The impedimetric biosensor is not used as much as the amperometric and potentiometric biosensors.

Electrochemical impedance spectroscopy (EIS) has many benefits in comparison with other electrochemical methods. During EIS experiments, a small amplitude ac signal is used to the system being deliberated. Consequently, it is a non-destructive technique for the evaluation of a wide range of materials. It can also afford detailed information of the systems under examination. EIS is an efficient analytical technique that enables scientists to effectively depict the real electrical and double-layer formation of an optimized electrode [16, 17]. The EIS technique, as a dominant method for analyzing electrochemical and electrical interfacial characteristics of a wide range of systems, is beneficial to control shifts in electrical features due to bio-recognition phenomena at the surfaces of modified electrodes [18-25]. By taking advantages of the EIS technique such as the capability to see electrode surface modifications just by looking impedance curves, and opportunity to design electrical circuit, according to obtained Nyquist plot, the impedimetric assessment exhibited excellent analytical performance toward the quantification analysis over the other electrical measurement techniques.

Nanostructured metal oxides have recently been used for fabrication of biosensing area, because of their ability to promote faster electron transfer between electrode and active site of the desired enzyme. Sensors which are based on metal oxides such as CuO or NiO [26] are highly sensitive, relatively cheap and enjoy the advantage of faster response as related to some specific nanostructures like nanorod, nanowire, nanoparticle, nanotube, and nano fiber [27-29]. The huge amount of copper oxide (CuO) found in nature and also its low cost of production, favorable electrochemical properties, and catalytic effects turn the copper oxide into one of the most appropriate metal oxides for optical, electrical, and photovoltaic applications, nonhomogeneous catalysis, magnetic storage devices, gas sensors, field-emission devices, lithium ion batteries, and etc [30-36]. Nanostructures of CuO might be produced by means of electrospinning [37, 38], argon sputtering [39], the low-temperature hydrothermal process [40-45], electrodeposition [46-50], pulsed laser deposition (PLD) [51], and chemically or electrochemically synthesis [52-56].

Chitosan, a (1→4)-2-amino-2-deoxy-β-D-glucan a derivative of chitin, is a linear hydrophilic polysaccharide that has received much attention in biological fields. It is an attractive biocompatible,

biodegradable and non-toxic nature biopolymer that has an excellent film-forming ability. In addition, chitosan can be used as a modification agent because it has abundant -NH_2 and -OH functional groups, which can react with bioactive molecules. Because of these characteristics, chitosan has been used as a substrate for the covalent immobilization of enzymes.

In the current investigation, CuO thin film as a unique transducer was fabricated on the conductive substrate of fluorinated-tin oxide (FTO) using reactive DC magnetron sputtering technique. GOx was covalently immobilized via chitosan on FTO/Nano-CuO to produce FTO/Nano-CuO/Chitosan/GOx biosensor. Measurement of glucose level was performed by using the advantage of glucose high affinity for interaction at the FTO/Nano-CuO/Chitosan/GOx biosensor and altering the charge transfer resistance at the surface of the electrode, which can be achieved through impedimetric assessment. The fabricated biosensor of FTO/Nano-CuO/Chitosan/GOx revealed a fast response time which was lower than 4 s, and high glucose detection sensitivity (0.261 kΩ per mM) at the range of 0.2–15 mM in phosphate buffer solutions (PBS, pH=7.4), and achieved favorable enzymatic performance for more than 4 weeks at the time being kept at the temperature of 4 °C when out of use.

2. Experimental

2.1. Materials and Methods

Fluorine-doped tin oxide (FTO) coated glass was purchased from Dyesol Company. D (+)-glucose (Merck 99.9%), glucose oxidase (GOx, G6125-10 KU from *Aspergillus Niger*, type II, 15,000-25,000 units/g Sigma-Aldrich), chitosan and the other compounds used in this study held high-grade analytical reagent and were purchased from Sigma-Aldrich. Double distilled de-ionized water was used for preparing all solutions throughout the experiments. All used solvents were obtained from Merck Company. Phosphate buffer solution (PBS) was prepared from KH_2PO_4 and K_2HPO_4 and the pH was set at 7.4. GOx solution was prepared in PBS for 4 h, 0.1 M, pH 7.4. A glucose stock solution was made in PBS of 0.1 M and kept at the temperature of 4 $^{\circ}$C. The glucose normal solutions with low concentrations were instantly prepared prior to the measurements. Nano-CuO thin films were deposited in a reactive DC

magnetron sputtering system (Nano-Structured Coatings Co., Tehran, Iran) by applying pure Cu target (99.999%) under various circumstances. The CuO thin films surface analysis was carried out using a Tescan Mira II FE-SEM at a voltage of 20.0 kV after coating the samples with a thin layer of gold by magnetron sputtering. Impedimetric and voltammetric experiments were conducted with a potentiostat/galvanostat (PGSTAT.302N, Autolab, Eco-Chemie, and The Netherlands). All electrochemical experiments were conducted in a usual system with three electrodes at ambient temperature. FTO/Nano-CuO/Chitosan/GOx electrode was used as a working electrode (surface area = 1 cm^2), and SCE and Pt electrodes were applied as reference and counter electrodes, respectively. The electrochemical cell was positioned in a Faraday cage to eliminate all stray effects of the environment. Peak-to-peak ac amplitude of 10 mV was used for the purpose of EIS measurements. A number of frequencies ranging from 100 kHz to 10 MHz were scanned, and the resistances were found. EIS data were analyzed by using Zview/Zplot (Scribner Associates, Inc.) based on the algorithm proposed by Macdonald (LEVM 7) and applying a complicated approximation method called the nonlinear least square method (CNLS) [57].

3. Results and discussion

3.1. Fabrication of FTO/Nano-CuO electrode by DC magnetron sputtering

One of the consistent procedures for production of nanostructured CuO was DC magnetron sputtering. The DC magnetron sputtering noteworthy advantage is that materials with high melting points are totally sputtered while these materials evaporation processes are challenging in a resistance evaporator. Sputtered CuO films have a configuration near to that of the target material. Sputtered CuO films characteristically have an enhanced adhesion than evaporated films. A target comprises a great material amount and is maintenance free. Sputtering targets comprise no hot parts. Innovative processes such as epitaxial growth are conceivable. In the light of this fact, DC magnetron sputtering delivers a homogeneous CuO media via high surface-to-volume ratio for efficient enzyme loading [58, 59].

In the current paper, DC magnetron sputtering has been applied in the atmosphere of Ar gas using DC power in order to produce FTO/Nano-CuO electrode. In the evacuated sputtering chamber, a 2 - inch plate of Cu-cathode was bombarded by ions of Ar^+ produced in the glow discharge plasma. In the reactive sputtering, a thin film is deposited and formed by chemical process occurring between the target compounds and a reactive gas injected into the vacuum environment [60]. The structure of thin film might be screened by changing the proportion of the reactive (O_2) and inert (Ar) gases.

In this paper, the sputtering circumstances are set to be the ideal ones for the emergence of Nano-CuO films with the least electrical resistivity. For the purpose of obtaining homogenous Nano-CuO film, four series of deposition processes were designed at various distances between target and substrate (4-9 cm), Ar: O_2 gases flow ratio (20:7, 20:6, 20:5, 20:4, 20:3, 20:2, 20:1 sccm/min), sputtering power (35-55 Watts) and deposition time (15-30 minutes). In each series of experiments, three sets were kept unchanged and only one set was altered to investigate the ideal circumstances. The first series which is shown in Fig. 1A refers to the relativity of the Nano-CuO films' electrical resistivity on distances between target and substrate (4-9 cm). The higher distances between target and substrate resulted in the higher electrical resistivity and the lower deposition rate of CuO nanoparticles; since in lower distances, Ar^+ with energy high levels harms the thin film of Nano-CuO. Fig. 1A reveals that a 5 cm distance between target and substrate is ideal for achieving a low electrical resistivity Nano-CuO film. The second series was related to the control of the flow ratio of Ar: O_2 gases as a crucial variable of reactive DC magnetron sputtering to obtain a less electrically resistant nanoporous CuO thin film. Our findings revealed that the level of oxygen found in gases flow ratio is a crucial factor involved in the emergence of CuO: Cu_2O phases in the thin film and it eventually outcomes in less or more electrical resistivity in the thin film. In this study, experimentally, we explored four experimental Ar: O_2 gases flow ratios (20:7, 20:6, 20:5, 20:4, 20:3, 20:2, 20:1 sccm/min). Gases flow ratios are important parameters to the formation of a uniform and porous thin layer. As seen in Fig. 1B, the 20:3 sccm/min Ar: O_2 gases flow ratio proved to be the most optimal condition for achieving the research purpose. The third series was the exploration of DC sputtering power that had a very strong effect on the Nano-CuO films' electrical resistivity (Fig. 1C). The

decreased DC sputtering power resulted in the decrease of Cu sputtered atoms from the target, and eventually raised the electrical resistivity of the thin film. As shown in Fig. 1C, the sputtering power less than 50 W led to the higher electrical resistivity of Nano-CuO thin film. Further, sputtering power more than 50 W led to the constancy and low electrical resistivity by increasing the amount of non-reacted Cu particles. Also, high sputtering power caused to higher outspread of Nano-CuO formation on the wrong place alliance to the substrate. As a result, we selected 50 W, as an optimum sputtering power option. The final investigation of ideal conditions was on the deposition time of the Nano-CuO (Fig. 1D). Based on the experimental results, the optimum deposition time for lower electrical resistivity and saving the energy was chosen about 20 minutes.

Figure 1 should be placed here

3.2. Fabrication of FTO/Nano-CuO/Chitosan/GOx biosensor

Enzymes immobilization is a noteworthy process in scheming the bio recognition part of enzyme based biosensors. Enzyme immobilization performs as the main factor to progress efficient biosensors with proper performances such as respectable operative and storage stability, great sensitivity, high selectivity, short response time and high reproducibility. Immobilized biomolecules have to keep their structure, their function, to preserve their biological activity after immobilization, to ensure firmly bound to the surface and not to be desorbed during the biosensor procedure. Taking maximum retaining biocatalyst specificity and analyte interaction and minimum loss of enzyme activity are determinative criteria in the assortment of enzyme immobilization protocol. Furthermore, an ideal biosensor has to be steady for long term application. Numerous immobilization strategies can be intended as adsorption, entrapment and encapsulation, covalence and cross-link. Covalent attachment of the biomolecule to the substrate is one of the most stylish immobilization methods accessible, although others as adsorption, entrapment and cross linking are repeatedly used.

For immobilization of GOx with chitosan, the chitosan was initially activated by exposing to a glutaraldehyde solution (1% w/v) for 1 h. Consequently, GOx solution (100 mg/mL) was prepared by dissolving 6 μL of stock glucose solution (50 mg/mL) in 10 μL of 0.05 mol/L buffer (pH 7.4), which corresponded to the optimum pH. The GOx solution was thoroughly mixed with the chitosan in the volume ratio of 1:20 and sonicated for 15 min. Then, 10 μL of the mixture was deposited on the surface of the FTO/Nano-CuO and allowed to evaporate at room temperature. Glutaraldehyde is worked as a cross linking agent between GOx and chitosan. One –CHO group of glutaraldehyde linked covalently to $–NH_2$ group of chitosan while other –CHO group is covalently linked to $–NH_2$ groups on the surface of GOx.

3.3. Optical transmission and morphological characterization of sputtered CuO thin film before and after enzyme immobilization

Fig. 2 displays the Nano-CuO thin film's ultraviolet transmission spectrum. The absorption onset and the excessive rates of transmission at wavelengths above 325 nm reveal the optical features and the low rates of diminutions like the Nano-CuO thin film' pits and voids. The CuO thin film hardness at the temperature of 400 °C resulted in a suitable conversion of the other component of Cu to CuO and a non-heterogeneously textured film which is demanded an enzyme immobilization in biosensor fabrication. Fig. 3 (A and B) illustrates the features of the surface structure of the thin film's nanoporous CuO at 2 μm and 200 nm magnifications by FE-SEM. The FE-SEM images proved the homogeneously extended surface and open pores which have a crucial role in enzymes immobilization strategy. Further, Fig. 3C exposes the biosensor surface upon enzyme immobilization, which clearly demonstrates high loading of the GOx enzyme on the electrode surface. The histogram of Nano-CuO particles size distribution was presented in Fig. 3D which was introduced the distribution of 50-60 nm CuO nanoparticle sizes. The EDX analysis shows the presence of CuO in the sputtered film before enzyme immobilization (Fig. 3E). The Au peaks are related to a thin Au layer which is covered with the film of FTO/Nano-CuO prior to FE-

SEM imaging for better electron conduction and resolution of FE-SEM images, and Sn and Si peaks illustrate the FTO substrate composition.

Figure 2 should be placed here

Figure 3 should be placed here

3.4. Study of GOx enzyme activity after immobilization

After enzyme immobilization, the electrical property of FTO/Nano-CuO/Chitosan/GOx was studied to determine the enzyme activity. For this measurement, a cell was made, which consists of gold wire (Φ 0.3 mm, 5 cm length) as an electrode and FTO/Nano-CuO/Chitosan/GOx as another electrode. Potential from 0.0-1.0 V was applied to the film and the corresponding DC current was measured [61]. For each sample, five series of measurement was performed at 25 °C which is an ambient temperature. Different concentrations of glucose solutions such as 0.2, 8, and 15 mM were made ready in 50 ml of PBS electrolyte. Fig. 4 (A, B) reveals the impact of glucose concentration. Prior to immobilization of enzyme, the electrode is not influenced by glucose concentration (Fig. 4A). Upon enzyme immobilization, the impact of the enhancement of glucose concentration is apparent and the voltage – current (I–V) curve's slope altered with an increase in the concentration of glucose (Fig. 4B). The I–V curve's slope (ΔI/ΔV) was applied as a means to measure the activity of biosensor enzyme and was obtained by using the following equation (1) [61-63]:

$$Sensitivity = \frac{\left(\frac{\Delta I}{\Delta V}\right)_x - \left(\frac{\Delta I}{\Delta V}\right)_0}{\left(\frac{\Delta I}{\Delta V}\right)_0} \quad (1)$$

Where $(\Delta I/\Delta V)_0$ shows the I–V curve's slope at glucose of '0' mM and $(\Delta I/\Delta V)_x$ is the slope of the I–V curve at glucose of 'x' mM, where x equals 0.2 - 15 mM of glucose.

Figure 4 should be placed here

3.5. Voltammetric and impedimetric characterization of FTO/Nano-CuO/Chitosan/GOx biosensor in the absence and presence of glucose

Cyclic voltammetry (CV) and electrochemical impedance spectroscopy (EIS) methods were exploited to monitor the procedure of FTO/Nano-CuO/Chitosan/GOx biosensor. Fig. 5A and B establish the CV studies and the impedance spectra in form of Nyquist plots (-Z'' *vs.* Z') studies at the time of the layer-based accumulation of FTO/Nano-CuO/Chitosan/GOx and their electrochemical features in glucose-free PBS containing 5.0 mM $[Fe(CN)_6]^{3-/4-}$ redox probe. The monitoring of layer by layer assembly of biosensor in the EIS spectrum and cyclic voltammogram is reflected by the appearance of a semicircle part corresponding to charge transfer resistance (R_{ct}) and magnitude of anodic peak current (i_{pa}) of a marker ($[Fe(CN)_6]^{3-/4-}$) in electrolyte solution, respectively.

Three layers of (a) FTO, (b) FTO/Nano-CuO, and (c) FTO/Nano-CuO/Chitosan/GOx result in a change of the electron transfer resistance and magnitude of anodic peak current from (a) i_{pa} = 0.09 mA, R_{ct} = 0.92 kΩ to (b) i_{pa} = 0.03 mA, R_{ct} = 1.86 kΩ and (c) i_{pa} = 0.01 mA, R_{ct} = 3.71 kΩ. Regarding the uncovered FTO electrode in PBS, the redox electrochemical peaks of $[Fe(CN)_6]^{3-/4-}$ might be observed obviously. Besides, the rate of R_{ct} is lower than that of the Nano-CuO film mainly due to the lower electrical resistivity of FTO (Fig. 5A and B; curve a,b). Upon the change in the loading of GOx onto FTO/Nano-CuO electrode, the i_{pa} value was lowered and the R_{ct} rate was improved (Fig. 5A and B; curve c). The elements of the suggested similar circuit model such as the constant phase element (CPE), the Warburg impedance (Z_w) and the solution resistance (R_s) are in the form of series, and the charge transfer resistance (R_{ct}) is paralleled with CPE (Fig. 5B, inset) [61,64]. Curves b and c in Fig. 5A and 5B demonstrate the CV and EIS representative spectra of the redox reaction of $[Fe(CN)_6]^{3-/4-}$ at two electrodes, namely FTO/Nano-CuO and FTO/Nano-CuO/Chitosan/GOx. As it can be perceived, GOx layer reduces direct transition of the electron with electrode substrate in comparison with Nano-CuO thin film because of its insulating character.

In the same manner, our categorized studies are followed at the surface of the FTO/Nano-CuO/Chitosan/GOx biosensor in the presence of glucose by determining the values of i_{pa} and R_{ct} through applying CV and EIS techniques (Fig. 6A and B). As three layers of electrode are assembled layer by layer, the rates of i_{pa} and R_{ct} is changed at the surface of Nano-CuO thin film and in relation to the uncovered FTO (i_{pa}= 0.07 mA, R_{ct}= 3.74 kΩ; curve b) that displays the appropriate transfer of electron at thin film of Nano-CuO due to the conductive nature of Cu [46,51]. Furthermore, after GOx immobilization onto the electrode, increasing in i_{pa} and decreasing in R_{ct} values (i_{pa}= 0.38 mA, R_{ct}= 1.12 kΩ; curve c) occurred which resulted in dealing and suitable electron transferring of glucose reaction by GOx enzyme.

Figure 5 should be placed here

Figure 6 should be placed here

As a result, the semiconductor surface is regarded as an appropriate matrix for designing new designs of the biosensor which facilitates the procedure of electron transfer. Transference of electron on the nanostructured CuO surface at the time of glucose measurement might be justified by using the procedure described below [65]:

$$Glucose + O_2 \xrightarrow{GOX} H_2O_2 + Gluconolactone \xrightarrow{H_2O} Gluconic\ acid \quad (2)$$

$$H_2O_2 \rightarrow 2H^+ + O_2 + 2e^- \quad (3)$$

After glucose oxidation by GOx, the H_2O_2 emergence and oxidize near the surface of the electrode, also the electrons produce after H_2O_2 oxidation and the excess electrons come back to the electrode surface and increase the conductivity of the electrode. The findings of CV and EIS data (Fig. 6 A, B) confirmed the sensing procedure described above.

For additional evidence to validate our proposed biosensing mechanism, the impedimetric response of FTO/Nano-CuO as a function of reducing (R) molecules (H_2O_2 in this project) concentration was measured in a glucose-free H_2O_2 solution. As shown in Fig. 7, the magnitude of R_{ct} decreases on the addition of H_2O_2 concentration from 0.001 to 0.009 M (a to i). When reducing molecules (R = H_2O_2) reacts, with pre-adsorbed negatively charged oxygen adsorbates (Eq. 2), the trapped electrons are given back to the conduction band of CuO, and as a result the decrease of R_{ct} is observed. The results obtained by impedimetric studies of R_{ct} variation as a function of H_2O_2 concentration support the proposed mechanism.

Figure 7 should be placed here

Fig. 8 illustrates a portrait of proposed process for the electrochemical reaction of glucose and GOx (equations 2 and 3) at the FTO/Nano-CuO/Chitosan/GOx electrode.

Figure 8 should be placed here

3.6. Effect of pH

The best buffer pH for glucose oxidizing process by GOx was deliberated as 7.4 at which GOx enzyme preserves its maximum activity and natural structure that is required in biological media to improve detection limit and sensitivity for glucose detection. The influence of pH on the electrochemical response of 0.6 mM of glucose on the surface of final FTO/Nano-CuO/Chitosan/GOx biosensor was explored in Fig. 9A.

3.7. Effect of salt concentration

The effect of the supporting electrolytes with various concentrations such as KI, KNO_3, $KClO_4$, and $NaNO_3$ on 0.6 mM glucose was likewise checked by the test solution. The supporting electrolytes concentration altered between 0.0 and 1.0 M in the test solution. The results presented that the method

sensitivity and peak current improved by rising KNO_3 salt concentration as a supporting electrolyte (Fig. 9B). The 1.0 M KNO_3 selected as finest concentration.

Figure 9 should be placed here

3.8. Impedimetric measurements' working curve

EIS affords label-free detection and is a sensitive indicator of an extensive variety of chemical and physical properties. An enhancing trend towards the growth of impedimetric biosensors is being presently detected. Impedimetric techniques have been achieved to illustrate the fabrication of the biosensors and to monitor the enzymes catalyzed reactions. Impedance spectroscopy delivers an effective technique to probe the electric features of surface-modified electrodes. During EIS experiments, a small amplitude ac signal is used to the system being deliberated. Consequently, it is a non-destructive technique for the evaluation of a wide range of materials. It can also afford detailed information of the systems under examination. The impedimetric assessments of the FTO/Nano-CuO/Chitosan/GOx biosensor have been extensively explored by various glucose amounts. As glucose concentration varies at the range of 0.2–15 mM (curve a to curve p), the R_{ct} value decreases significantly (Fig. 10A). Our results expose that the biosensor of this investigation which is based on a porous semi conductive matrix of Nano-CuO, with low mass transfer barrier, constitutes a proper media for quick electron transferring without reducing the enzyme activity. The calibration curve was drawn for several glucose concentrations (0.2–15 mM) at the FTO/Nano-CuO/Chitosan/GOx biosensor by registering its R_{ct} variations ($|\Delta R_{ct}| = |R_{ct\ glucose} - R_{ct\ buffer\ (blank)}|$). The linear scale was attained [ΔR_{ct} (kΩ) = 0.306 (±0.027) + 0.261 (±0.003) × [glucose] (mM); R^2= 0.9981] as perceived in Fig. 10B. The FTO/Nano-CuO/Chitosan/GOx biosensor displays detection limit of 27 µM for glucose and sensitivity of 0.261 kΩ per mM with a linear range falling in the 0.2–15 mM range. Ultimately, this report based on impedimetric research reveals the possibility of using this electrochemical procedure and endorses the fundamental catalytic role of the immobilized enzymes in the glucose recognition and determination. From impedimetric studies, it is confirmed that the developed

biosensors can be reused. The current study biosensor obviously displays outstanding detection limit and response time.

Figure 10 should be placed here

3.9 Human serum sample and selectivity study

The precise selection of FTO/Nano-CuO/Chitosan/GOx biosensor for the purpose of glucose measurement has been examined using EIS studies through distinctly combining normal concentrations of some interferents found in human serum such as uric acid (0.05 mM), ascorbic acid (0.1 mM), and cysteine (0.05 mM) with glucose (0.2 mM). The EIS analysis of all the mentioned interferents was presented in Fig. 11. The R_{ct} value was achieved as ($R_{ct\ (mix)}$ - $R_{ct\ (gl)}$ / $R_{ct\ (gl)}$, where $R_{ct\ (mix)}$ and $R_{ct\ (gl)}$ were charge transfer resistance of glucose combined with interferents and charge transfer resistance of glucose alone. The outcomes of this investigation display the existence of the highest level of interference in the recognition of glucose with uric acid, ascorbic acid and cysteine have interference rates of 3.1%, 1.4%, and 2.5%, correspondingly. The results expose the significance of the created biosensor in the precise of glucose detection.

Numerous experiments were directed on blood serums to examine the reliability of the FTO/Nano-CuO/Chitosan/GOx biosensor. The concentration of glucose was determined by using the calibration curve (Table 1). Some related experiments were done by using spectrophotometer in a local clinical laboratory. The findings exposed the existence of a high level of consistency and precision between the two procedures and demonstrated that the proposed biosensor can be successfully employed to human serum samples with high accuracy and precision. The fabricated FTO/Nano-CuO/Chitosan/GOx biosensor has revealed a quick response time, shorter than 4 s, and has reserved a high level of enzymatic activity for a time period longer than four weeks at the temperature of 4 °C and at the time being out of use. By way of conclusion, the life test study was measured by investigation of the oxidation peak current response of FTO/Nano-CuO/Chitosan/GOx biosensor in the presence of glucose at various periodic times.

As Fig. 12 indicates, upon GOx immobilization, the biosensor exploited in this study kept 87.5% of its bioactivity during thirty-fifth days.

Table 2 illustrates the comparison between some characterizations of the FTO/Nano-CuO/Chitosan/GOx biosensor and the other developed glucose enzymatic/nonenzymatic sensors based on CuO layer. The biosensor employed in the present study perceptibly demonstrates the high dynamic range, response time, and detection limit as an impedimetric enzymatic biosensor compared with the findings reported in the formerly published kinds of literature. The biosensor dynamic range based on the value of the V_m (Maximal velocity) and K_m (Michaelis constant) which depend on the enzyme loading. In this project, exploiting nanoporous thin film as a family of the richest nanostructure with more active sites for enzyme loading enhanced dynamic range by increasing K_m and V_m.

Figure 11 should be placed here

Table 1 should be placed here

Figure 12 should be placed here

Table 2 should be placed here

4. Conclusions

In the present study, a facile and simple fabrication method of a semiconductor based glucose biosensor was reported. The application of biosensor is dependent on (i) the rate of immobilized enzyme, which relates to the surface area/volume ratio and morphology of the matrix, and (ii) the porosity of matrix which is providing rapid diffusion from solution to the immobilized enzyme. In the present paper, Nano-CuO thin film, which is fabricated by reactive DC sputtering system, with a good level of homogeneity of the nanoporous structure was employed for developing an electrochemical glucose biosensor through covalent GOx immobilization. The developed biosensor had revealed high sensitivity,

broad dynamic range, low detection limit, good stability, quick response time, and long-term reproducibility. These features are conceivable due to retaining enzyme activity as a result of the suitable immobilization of GOx in the nanoporous thin film made of nanostructured CuO which prepares a bigger surface area, facilitates enzyme loading, and decreases the substrate's diffusion distance to reach the immobilized enzyme. Also, the impedimetric analysis presented a quick response time of shorter than 4 s accompanied with a broad dynamic range of 0.2–15 mM, good sensitivity (0.261 kΩ per mM) and detection limit of 27 μM for glucose.

Acknowledgement

S. A. Mozaffari acknowledges the support rendered by the Iranian Research Organization for Science and Technology (IROST), Iran Nanotechnology Initiative Council (INIC) and Nanostructured Coating Co. for this research.

References

[1] J. Wang, Electrochemical glucose biosensors, Chem. Rev. 108 (2008) 814–825.

[2] S.A. Zaidi, J.H. Shin, Recent developments in nanostructure based electrochemical glucose sensors, Talanta 149 (2016) 30–42.

[3] H. Zhu, L. Li, W. Zhou, Z. Shao, X. Chen, Advances in non-enzymatic glucose sensors based on metal oxides, J. Mater. Chem. B 4 (2016) 7333–7349.

[4] J.R. Gavin, The Importance of monitoring blood glucose. In US endocrine disease 2007, Touch briefings: Atlanta, GA, USA, 2007; 1–3.

[5] L. Shabnam, S.N. Faisal, A.K. Roy, E. Haque, A.I. Minett, V.G. Gomes, Dope graphene/Cu nanocomposite: A high sensitivity non-enzymatic glucose sensor for food, Food Chemistry 221 (2017) 751–759.

[6] J. Wang, Carbon-nanotube based electrochemical biosensors: A review, Electroanalysis 17 (2005) 7–14.

[7] G.A. Rivas, M.D. Rubianes, M.C. Rodriguez, N.F. Ferreyra, G.L. Luque, M.L. Pedano, S.A. Miscoria, C. Parrado, Carbon nanotubes for electrochemical biosensing, Talanta 74 (2007) 291-307.

[8] Y. Lin, F. Lu, Y. Tu, Z. Ren, Glucose biosensors based on carbon nanotube nanoelectrode ensembles, Nano Lett. 4 (2004) 191-195.

[9] C. Li, Y. Liu, L. Li, Z. Du, S. Xu, M. Zhang, X. Yin, T. Wang, A novel amperometric biosensor based on NiO hollow nanospheres for biosensing glucose, Talanta 77 (2008) 455-459.

[10] Y. Wang, H. Xu, J. Zhang, G. Li, Electrochemical sensors for clinic analysis, Sensors 8 (2008) 2043–2081.

[11] M.A. Morikawa, N. Kimizuka, M. Yoshihara, T. Endo, New colorimetric detection of glucose by means of electron-accepting indicators: ligand substitution of $[Fe(acac)_3^{-n}(phen)_n]^{n+}$ complexes triggered by electron transfer from glucose oxidase, Chem. Eur. J. 8 (2002) 5580–5584.

[12] Y. Miwa, M. Nishizawa, T. Matsue, I. Uchida, A conductometric glucose sensor based on a twin-microband electrode coated with a polyaniline thin film, Bull. Chem. Soc. Japan 67 (1994) 2864–2866.

[13] S. Mansouri, J.S. Schultz, A miniature optical glucose sensor based on affinity binding, Nat. Biotechnol. 2 (1984) 885–890.

[14] S.K. Shukla, M.M. Demir, P.P. Govender, A. Tiwari, S.K. Shukla, Optical fibre based non-enzymatic glucose sensing over Cu^{2+}-dopedpolyaniline hybrid matrix, Sens. Actuators B: Chem 242 (2017) 522–528.

[15] J.C. Pickup, F. Hussain, N.D. Evans, O.J. Rolinski, D.J. Birch, Fluorescence-based glucose sensors, Biosens. Bioelectron. 20 (2005) 2555–2565.

[16] J.G. Guan, Y.Q. Miao, Q.J. Zhang, Impedimetric biosensor, J. Biosci. Bioeng. 97 (2004) 219–226.

[17] C.I.L. Justino, A.C. Duarte, T.A.P. Rocha-Santos, Critical overview on the application of sensors and biosensors for clinical analysis, TrAC, Trends Anal. Chem. 85 (2016) 30–36.

[18] K. Fuchs, U. Kaatze, Molecular dynamics of carbohydrate aqueous solutions. Dielectric relaxation as a function of glucose and fructose concentration. J. Phys. Chem., Sect. B 105 (2001) 2036–2042.

[19] A. Caduff, E. Hirt, Y. Feldman, Z. Ali, L. Heinemann, First human experiments with a novel non-invasive, non-optical continuous glucose monitoring system, Biosens. Bioelectron. 19 (2003) 209–217.

[20] R. Rahmanian, S.A. Mozaffari, H. Salar Amoli, M. Abedi, Development of sensitive impedimetric urea biosensor using DC sputtered Nano-ZnO on TiO_2 thin film as a novel hierarchical nanostructure transducer, Sensors and Actuators B 256 (2018) 760–774.

[21] S.A. Mozaffari, M. Ranjbar, E. Kouhestanian, H. Salar Amoli, M.H. Armanmehr, An investigation on the effect of electrodeposited nanostructured ZnO on the electron transfer process efficiency of TiO_2 based DSSC, Mater. Sci. Semicond. Process 40 (2015) 285–292.

[22] R. Shabani, S.A. Mozaffari, S.W. Husain, M. Saber Tehrani, Selective nanosensing of copper (II) ion using L-Lysine in-situ functionalized gold cysteamine self-assembled monolayer, Iran. J. Sci. Technol. 33 (2009) 335–347.

[23] R.K. Shervedani, S.A. Mozaffari, Copper (II) nanosensor based on a gold cysteamine self-assembled monolayer functionalized with salicylaldehyde, Anal. Chem. 78 (2006) 4957–4963.

[24] S.A. Mozaffari, T. Chang, S.M. Park, Diffusional electrochemistry of cytochrome c on mixed captopril/3- mercapto-1-propanol self-assembled monolayer modified gold electrodes, J. Phys. Chem. C 113 (2009) 12434–12442.

[25] S.A. Mozaffari, T. Chang, S.M. Park, Self-assembled monolayer as a pre-concentrating receptor for selective serotonin sensing, Biosens. Bioelectron. 26 (2010) 74–83.

[26] P. Naderi Asrami, M. Saber Tehrani, P. Aberoomand Azar, S.A. Mozaffari, Impedimetric glucose biosensor based on nanostructure nickel oxide transducer fabricated by reactive RF magnetron sputtering system, J. Electroanal. Chem. 801 (2017) 258–266.

[27] Z. Zhu, L.G. Gancedo, A. J. Flewitt, H. Xie, F. Moussy, W.I. Milne, A critical review of glucose biosensors based on carbon nanomaterials: Carbon nanotubes and graphene, Sensors 12 (2012) 5996-6022.

[28] S.I. Mho, D.C. Johnson, Electrocatalytic Response of Carbohydrates at Copper-Alloy Electrodes, J. Electroanal. Chem. 500 (2001) 524–532.

[29] A. Salimi, M. Roushani, Non-enzymatic glucose detection free of ascorbic acid interference using nickel powder and nafion sol–gel dispersed renewable carbon ceramic electrode, Electrochem. Commun. 7 (2005) 879–887.

[30] X. Jiang, T. Herricks, Y. Xia, CuO nanowires can be synthesized by heating copper substrates in air, Nano Lett. 2 (2002) 1333–1338.

[31] D. Wang, C. Song, Z. Hu, X. Fu, Fabrication of hollow spheres and thin films of nickel hydroxide and nickel oxide with hierarchical structures, J. Phys. Chem. B 109 (2005) 1125–1129.

[32] R.P. Wijesundera, M. Hidaka, K. Koga, J.Y. Choi, N.E. Sung, Structural and electronic properties of electrodeposited heterojunction of CuO/Cu_2O, Ceram. Silik. 54 (2010) 19–25.

[33] C. Dong, X. Xing, N. Chen, X. Liu, Y. Wang, Biomorphic synthesis of hollow CuO fibers for low-ppm-level n-propanol detection via a facile solution combustion method, Sens. Actuators B: Chem 230 (2016) 1–8.

[34] X.P. Gao, J.L. Bao, G.L Pan, H.Y. Zhu, P.X. Huang, F. Wu, D.Y. Song, Preparation and electrochemical performance of polycrystalline and single crystalline CuO nanorods as anode materials for Li ion battery, J. Phys. Chem. B 108 (2004) 5547–5551.

[35] J. Zhang, J. Liu, Q. Peng, X. Wang, Y. Li, Nearly monodisperse Cu_2O and CuO nanospheres: Preparation and applications for sensitive gas sensors, Chem. Mater. 18 (2006) 867–871.

[36] A.E. Rakhshani, Y. Makdisi, X. Mathew, Deep energy levels and photoelectrical properties of thin cuprous oxide films, Thin Solid Films 288 (1996) 69–75.

[37] W. Wang, Z. Li, W. Zheng, J. Yang, H. Zhang, C. Wang, Electrospun palladium (IV)-doped copper oxide composite nanofibers for non-enzymatic glucose sensors, Electrochem. Commun. 11 (2009) 1811–1814.

[38] W. Wang, L. Zhang, S. Tong, X. Li, W. Song, Three-dimensional network films of electrospun copper oxide nanofibers for glucose determination, Biosens. Bioelectron. 25 (2009) 708–714.

[39] G. Panzner, B. Egert, H.P. Schmidt, The stability of CuO and Cu_2O surfaces during argon sputtering studied by XPS and AES, Surf. Sci. 151 (1984) 400–408.

[40] C.B. McAuley, Y. Du, G.G. Wildgoose, R.G. Compton, The use of copper(II) oxide nanorod bundles for the non-enzymatic voltammetric sensing of carbohydrates and hydrogen peroxide, Sens. Actuators B: Chem 135 (2008) 230–235.

[41] A. Umar, M.M. Rahman, A. Al-Hajry, Y.B. Hahn, Enzymatic glucose biosensor based on flower-shaped copper oxide nanostructures composed of thin nanosheets, Electrochem. Commun. 11 (2009) 278–281.

[42] E. Reitz, W. Jia, M. Gentile, Y. Wang, Y. Lei, CuO nanospheres based nonenzymatic glucose sensor, Electroanalysis 20 (2008) 2482 – 2486.

[43] M.U. Prathap, B. Kaur, R. Srivastava, Hydrothermal synthesis of CuO micro-/nanostructures and their applications in the oxidative degradation of methylene blue and non-enzymatic sensing of glucose/H_2O_2, J. Colloid Interface Sci. 370 (2012) 144–154.

[44] X. Ji, A. Wang, Q. Zhao, Direct growth of copper oxide films on Ti substrate for nonenzymatic glucose sensors, J. of Nanomaterials, 2014 (2014) 287303–287308.

[45] Z.H. Ibupoto, K. Khun, V. Beni, X. Liu, M. Willander, Synthesis of novel CuO nanosheets and their non- enzymatic glucose sensing applications, Sensors 13 (2013) 7926-7938.

[46] J. Yang, L.C. Jiang, W.D. Zhang, S. Gunasekaran, A highly sensitive non-enzymatic glucose sensor based on a simple two-step electrodeposition of cupric oxide (CuO) nanoparticles onto multi-walled carbon nanotube arrays, Talanta 82 (2010) 25–33.

[47] J. Yang, W.D. Zhang, S. Gunasekaran, An amperometric non-enzymatic glucose sensor by electrodepositing copper nanocubes onto vertically well-aligned multi-walled carbon nanotube arrays, Biosens. Bioelectron. 26 (2010) 279–284.

[48] P.M. Nia, W.P. Meng, F. Lorestani, M.R. Mahmoudian, Y. Alias, Electrodeposition of copper oxide/polypyrrole/reduced graphene oxide as a nonenzymatic glucose biosensor, Sens. Actuators B: Chem 209 (2015) 100–108.

[49] H.Y. Yu, M.Q. Xu, S.H. Yu, G.C. Zhao, A novel non-enzymatic glucose sensor based on CuO-graphene nanocomposites, Int. J. Electrochem. Sci. 8 (2013) 8050–8057.

[50] Kh. Ghanbari, Z. Babaei, Fabrication and characterization of non-enzymatic glucose sensor based on ternary NiO/CuO/polyaniline nanocomposite, Anal. Biochem. 498 (2016) 37–46.

[51] N. Batra, M. Tomar, V. Gupta, ZnO–CuO composite matrix based reagentless biosensor for detection of total cholesterol, Biosens. Bioelectron. 67 (2015) 263–271.

[52] Y. Li, F. Huang, J. Chen, T. Mo, S. Li, F. Wang, S. Feng, Y. Li, A high performance enzyme-free glucose sensor based on the graphene-CuO nanocomposites, Int. J. Electrochem. Sci. 8 (2013) 6332 – 6342.

[53] A. Uzunoglu, L.A. Stanciu, Novel CeO_2–CuO-decorated enzymatic lactate biosensors operating in low oxygen environments, Anal. Chim. Acta 909 (2016) 121–128.

[54] B. Wang, Y. Wu, Y. Chen, B. Weng, C. Li, Flexible paper sensor fabricated via in situ growth of Cu nanoflower on RGO sheets towards amperometrically non-enzymatic detection of glucose, Sens. Actuators B: Chem 238 (2017) 802–808.

[55] X.W. Liu, P. Pan, Z.M. Zhang, F. Guo, Z.C. Yang, J.Wei, Z. Wei, Ordered self-assembly of screen-printed flower-like CuO and CuO/MWCNTs modified graphite electrodes and applications in non-enzymatic glucose sensor, J. Electroanal. Chem. 763 (2016) 37–44.

[56] L. Shabnam, S.N. Faisal, A.K. Roy, A.I. Minett, V.G. Gomes, Nonenzymatic multispecies sensor based on Cu-Ni nanoparticle dispersion on doped graphene, Electrochim. Acta 224 (2017) 295–305.

[57] J.R. Macdonald, J. Schoonman, A.P. Lehnen, The applicability and power of complex nonlinear least squares for the analysis of impedance and admittance data, J. Electroanal. Chem. 131 (1982) 77–95.

[58] O. Baghriche, C. Ruales, R. Sanjines, C. Pulgarin, A. Zertal, I. Stolitchnov, J. Kiwi, Ag-surfaces sputtered by DC and pulsed DC-magnetron sputtering effective in bacterial inactivation: testing and characterization, Surf. Coat. Technol. 206 (2012) 2410–2416.

[59] P.J. Kelly, R.D. Arnell, Magnetron sputtering: A review of recent developments and applications, Vacuum 56 (2000) 159–172.

[60] L.R. Yao, F.H. Lu, Low vacuum deposition of aluminum nitride thin films by sputtering, International Journal of Applied Ceramic Technology 10 (2013) 51–59.

[61] S.A. Mozaffari, R. Rahmanian, M. Abedi, H. Salar Amoli, Urea impedimetric biosensor based on reactive RF magnetron sputtered zinc oxide nanoporous transducer, Electrochim. Acta 146 (2014) 538–547.

[62] S.G. Ansari, Z. Ansari, R.Wahab, Y.S. Kim, G. Khang, H.S. Shin, Glucose sensor based on nano-baskets of tin oxide templated in porous alumina by plasma enhanced CVD, Biosens. Bioelectron. 23 (2008) 1838–1842.

[63] S.K. Mahadeva, J. Kim, Conductometric glucose biosensor made with cellulose and tin oxide hybrid nanocomposite, Sens. Actuators B: Chem 157 (2011) 177–182.

[64] R. Rahmanian, S.A. Mozaffari, Electrochemical fabrication of ZnO-polyvinyl alcohol nanostructured hybrid film for application to urea biosensor, Sens. Actuators B: Chem 207 (2015) 772–781.

[65] E.H. Yoo, S.Y. Lee, Glucose biosensors: An overview of use in clinical practice, Sensors 10 (2010) 4558– 4576.

[66] Z. Zhuang, X. Su, H. Yuan, Q. Sun, D. Xiao, M.M. Choi, An improved sensitivity non-enzymatic glucose sensor based on a CuO nanowire modified Cu electrode, Analyst 133 (2008) 126–132.

[67] L.C. Jiang, W.D. Zhang, A highly sensitive nonenzymatic glucose sensor based on CuO nanoparticles- modified carbon nanotube electrode, Biosens. Bioelectron. 25 (2010) 1402–1407.

Figure captions

Fig. 1. Effect of **(A)** target-to-substrate distance, **(B)** Ar: O_2 gases flow ratio, **(C)** sputtering power, and **(D)** deposition time on FTO/Nano-CuO electrode electrical resistivity.

Fig. 2. UV transmission spectrum of FTO/Nano-CuO film.

Fig. 3. (A-B) FE-SEM images of Nano-CuO film deposited at various magnifications, **(C)** FTO/Nano-CuO/Chitosan/GOx electrode upon immobilization of enzyme, **(D)** histogram of Nano-CuO particle size, **(E)** EDX analysis of FTO/Nano-CuO electrode, where the EDX Au peaks are related to a thin Au layer which is covered with the film of FTO/Nano-CuO prior to SEM imaging for achieving higher electron conduction of electron and better resolution of FE-SEM images.

Fig. 4. I–V curves demonstrating the influence of the immobilization of glucose oxidase on FTO/Nano-CuO film with the incremental concentration of glucose, **(A)** prior to and **(B)** upon GOx immobilization.

Fig. 5. (A) Cyclic voltammogram achieved in glucose-free PBS (pH 7.4) containing 5.0 mM $[Fe(CN)_6]^{3-/4-}$ on FTO (a), FTO/Nano-CuO (b), and FTO/Nano-CuO/Chitosan/GOx (c) at the scan rate of 0.05 V/s. **(B)** The Nyquist plots (-Z'' *vs.* Z') found by measurements of the Faradaic impedance in glucose-free PBS (pH 7.4) containing 5.0 mM $[Fe(CN)_6]^{3-/4-}$ on FTO (a), FTO/Nano-CuO (b), and FTO/Nano-CuO/Chitosan/GOx (c). The inset in (**B**) shows the modified Randles equivalent circuit.

Fig. 6. (A) Cyclic voltammogram achieved at 0.05 V/s scan rate in PBS (pH 7.4) containing 0.6 mM glucose in the lack of $[Fe(CN)_6]^{3-/4-}$ probe on FTO (a), FTO/Nano-CuO (b), and FTO/Nano-CuO/Chitosan/GOx (c). **(B)** The Nyquist plots (-Z'' *vs.* Z') obtained by measuring the rate in PBS (pH 7.4) containing 0.6 mM glucose without using $[Fe(CN)_6]^{3-/4-}$ probe on FTO (a), FTO/Nano-CuO (b) and FTO/Nano-CuO/Chitosan/GOx (c).

Fig. 7. Fig. The Nyquist plots (-Z'' *vs.* Z') obtained on the FTO/Nano-CuO electrode in the presence of different concentration of H_2O_2.

Fig. 8. Portrait of the mechanistic model suggested for transferring electrons at the FTO/Nano-CuO/Chitosan/GOx biosensor in the presence of glucose in PBS (pH 7.4).

Fig. 9. Effect of **(A)** pH and **(B)** KNO_3 salt concentration on FTO/Nano-CuO/Chitosan/GOx biosensor 0.6 mM glucose response.

Fig. 10. (A) The Nyquist plots (-Z'' *vs.* Z') achieved on the FTO/Nano-CuO/Chitosan/GOx biosensor with different concentrations of glucose (0.2-15 mM). **(B)** Different amounts of charge transfer resistance (R_{ct}) that follow glucose concentration, shows calibration curve.

Fig. 11. The diagram demonstrates the impact interferents have on the response rate of FTO/Nano-CuO/Chitosan /GOx biosensor (AA = Ascorbic acid, UA = Uric acid).

Fig. 12. Conduction of the life test on the response time of the oxidation peak current of 0.6 mM glucose on FTO/Nano-CuO/Chitosan/GOx biosensor.

Tables

Table 1. Measurement of the level of glucose in blood serum.

Method	**Sample number**				
	1	**2**	**3**	**4**	**5**
Determination by Spectrophotometry (mM)	5.43	5.05	4.60	9.21	5.10
Determination by FTO/Nano-CuO/Chitosan/GOx **biosensor (mM)**	5.53	5.27	4.90	8.80	5.31
R.S.D.[a] (n=5) (%)	2.8	1.5	3.2	2.5	1.7

R.S.D.[a] : Relative Standard Deviation

Table 2. Analytical features of FTO/Nano-CuO/Chitosan/GOx biosensor compare with the other developed enzymatic and nonenzymatic glucose sensor/biosensor based on CuO.

Electrode matrix	D.L. (nM/µM)	D.R. (µM/mM)	R.T. (Sec)	Detection method	type of sensor	Ref.
flower-shaped CuO	1.37 µM	0.01 – 10 mM	5 sec	Amperometric	Enzymatic	[54]
CuO / Ti	2 µM	-	2 sec	Amperometric	Nonenzymatic	[57]
Cu_xO/Ppy/rGO	0.03 µM	-	-	Amperometric	Nonenzymatic	[61]
CuO/graphene	1 µM	1 µM-8 µM	-	Amperometric	Nonenzymatic	[62]
ZnO – CuO	0.038 µM	0.1 -4167 µM	-	Amperometric	Nonenzymatic	[64]
CuO nanowire	49 nM	0.4 – 2 mM	-	Amperometric	Nonenzymatic	[78]
MWNTs/CuO nanoparticle	0.2 µM	Up to 1.2 mM	1 sec	Amperometric	Nonenzymatic	[79]
FTO/Nano-CuO/Chitosan/GOx	27 µM	0.2-15 mM	4 sec	Impedimetric	Enzymatic	This work

Detection Limit [D.L.], Detection Range [D.R.], Response Time [R.T.].

Highlights

- Application of reactive DC magnetron sputtering as a promising technique for fabrication of nanostructured CuO semi-conductor as an efficient transducer.

- Fabrication of a novel disposable impedimetric glucose biosensor based on Nano-CuO porous thin film as an appropriate media with a high area to volume ratio for enzyme immobilization.

- High stability of enzyme by successful immobilization via chitosan bonding.

- Impedimetric assessments for glucose monitoring because of good sensitivity, rapidity and repeatability.

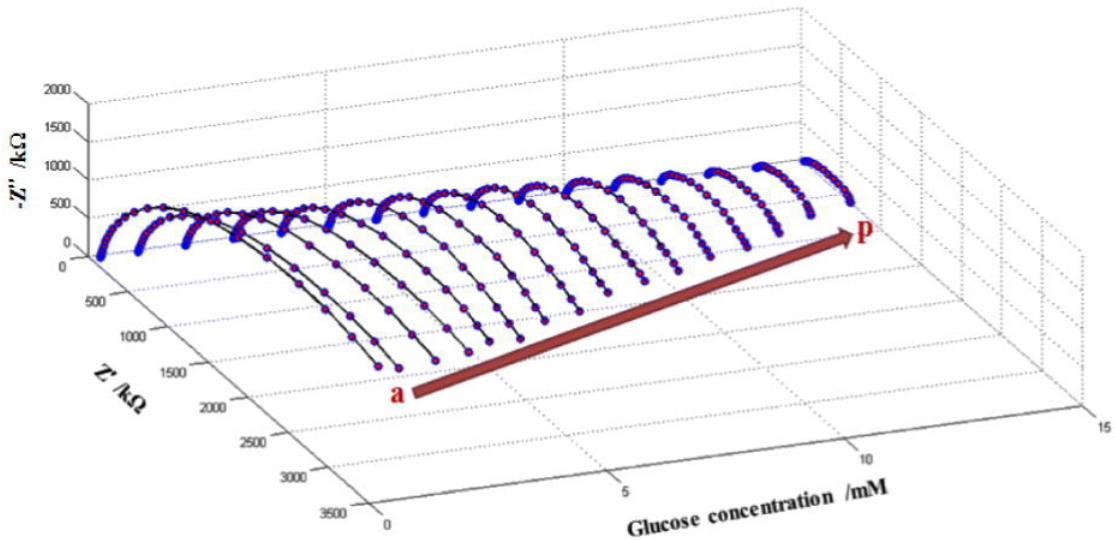

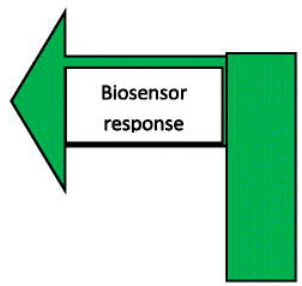

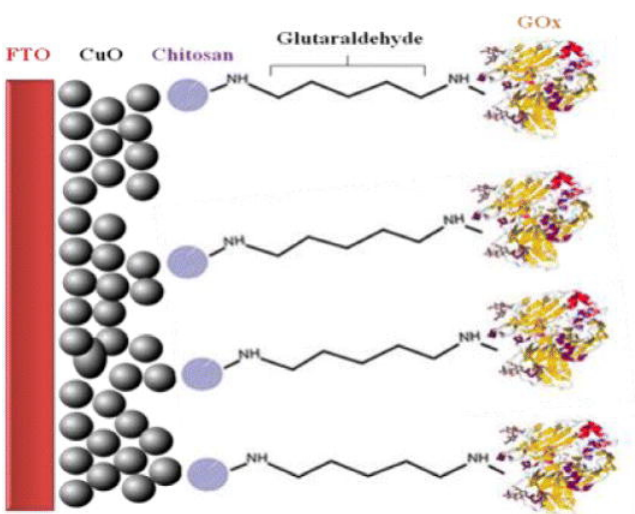

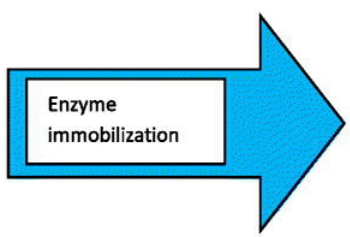

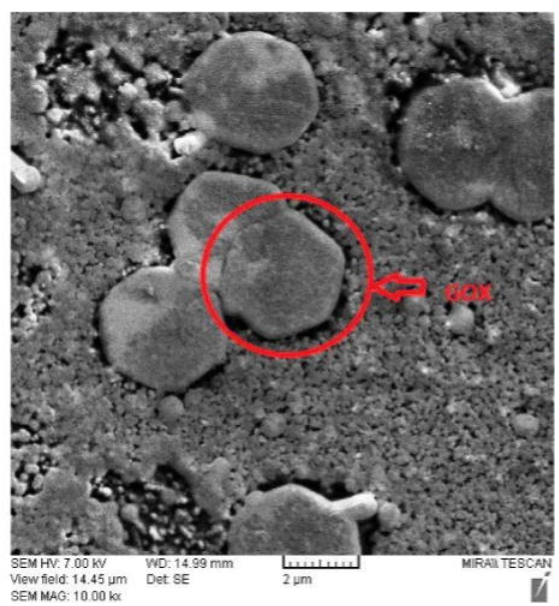

Graphics Abstract

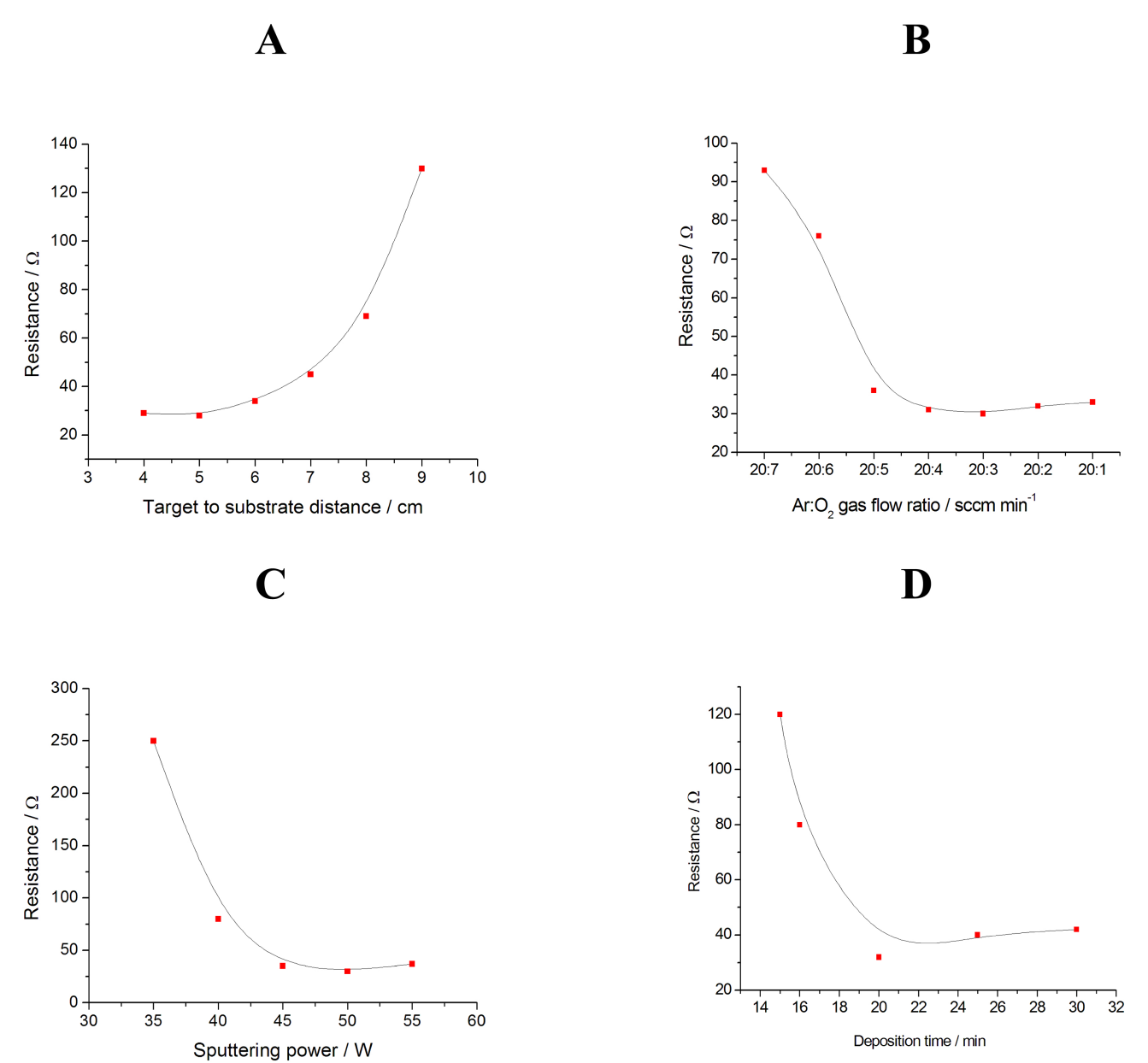
A
Resistance / Ω
Target to substrate distance / cm
B
Resistance / Ω
Ar:O2 gas flow ratio / sccm min-1
20:7
20:6
20:5
20:4
20:3
20:2
20:1
C
Resistance / Ω
Sputtering power / W
D
Resistance / Ω
Deposition time / min

Figure 1

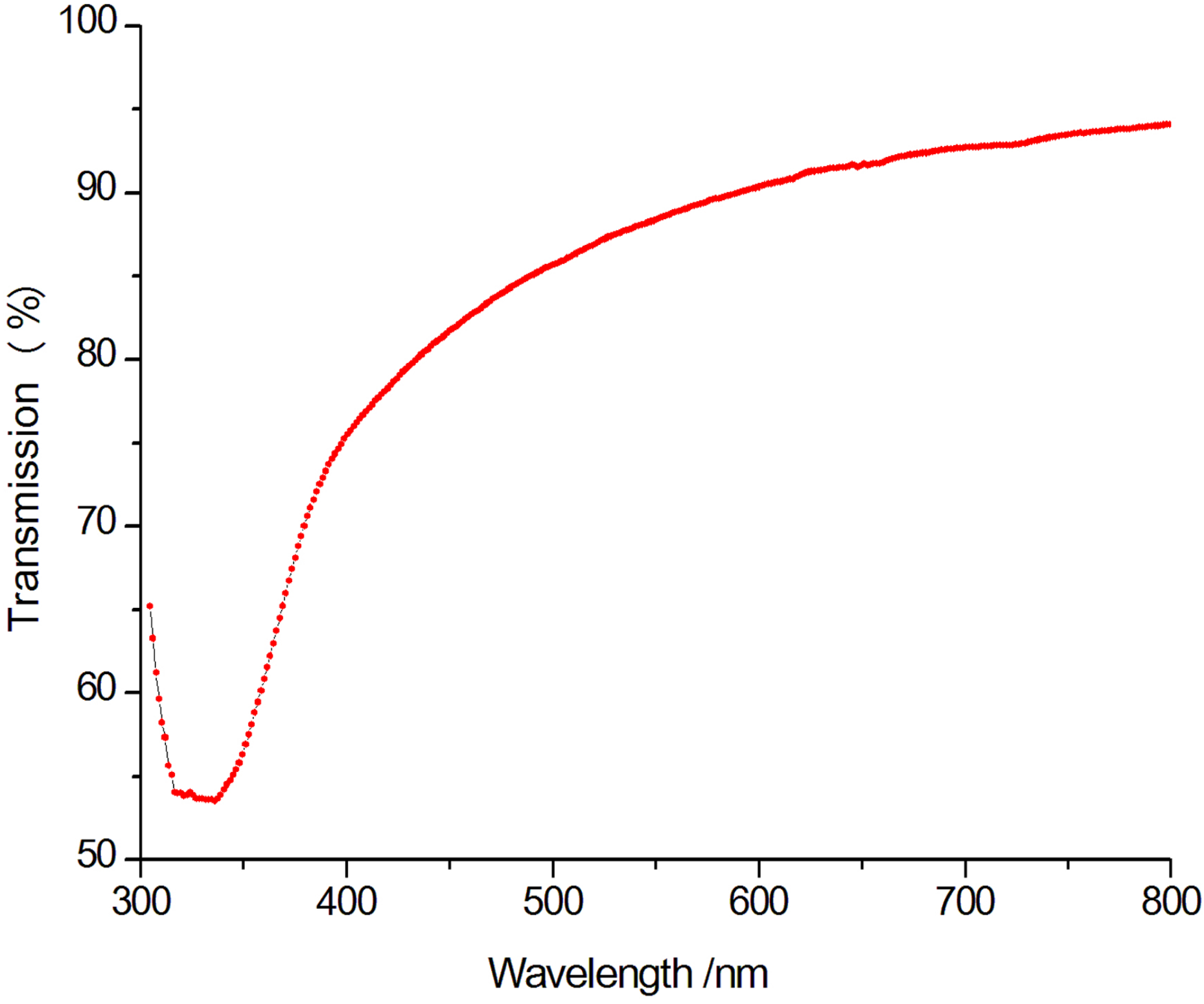
100
90
80
70
60
50
Transmission (%)
300
400
500
600
700
800
Wavelength /nm

Figure 2

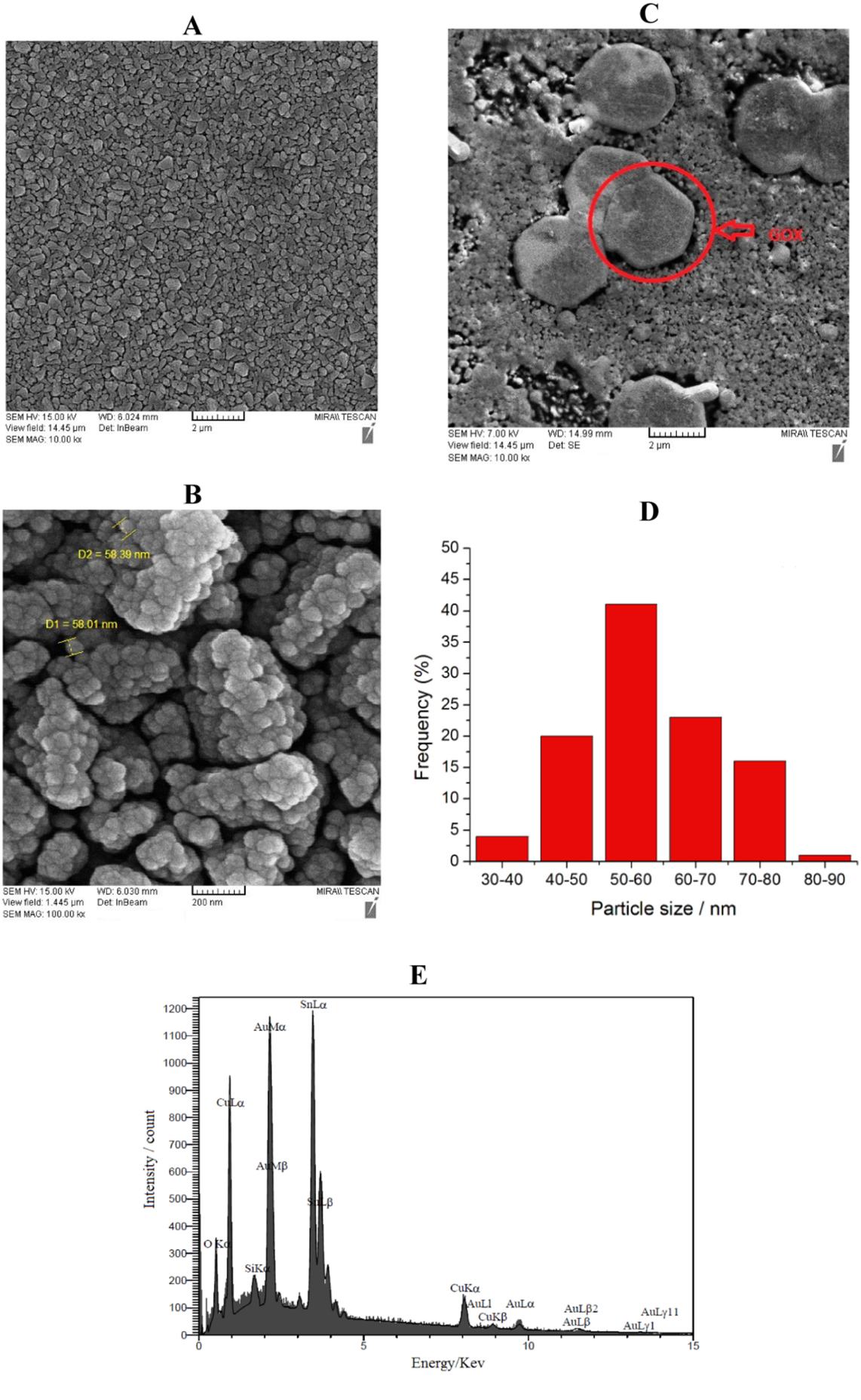
A
SEM HV: 15.00 kV
View field: 14.45 μm
SEM MAG: 10.00 kx
WD: 6.024 mm
Det: InBeam
2 μm
MIRA\\ TESCAN
C
GOX
SEM HV: 7.00 kV
View field: 14.45 μm
SEM MAG: 10.00 kx
WD: 14.99 mm
Det: SE
2 μm
MIRA\\ TESCAN
B
D2 = 58.39 nm
D1 = 58.01 nm
SEM HV: 15.00 kV
View field: 1.445 μm
SEM MAG: 100.00 kx
WD: 6.030 mm
Det: InBeam
200 nm
MIRA\\ TESCAN
D
Frequency (%)
Particle size / nm
30-40
40-50
50-60
60-70
70-80
80-90
E
Intensity / count
Energy/Kev
SnLα
AuMα
CuLα
AuMβ
SnLβ
O Kα
SiKα
CuKα
AuL1
CuKβ
AuLα
AuLβ2
AuLβ
AuLγ11
AuLγ1

Figure 3

A

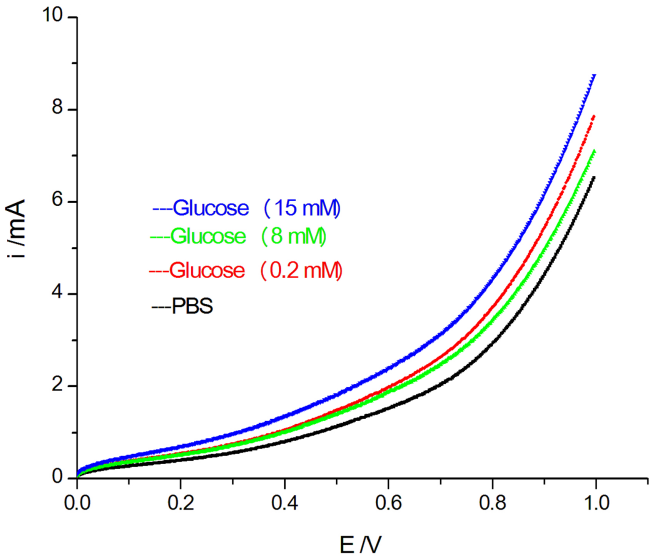
10
8
6
4
2
0
i /mA
---Glucose (15 mM)
---Glucose (8 mM)
---Glucose (0.2 mM)
---PBS
0.0
0.2
0.4
0.6
0.8
1.0
E /V

B

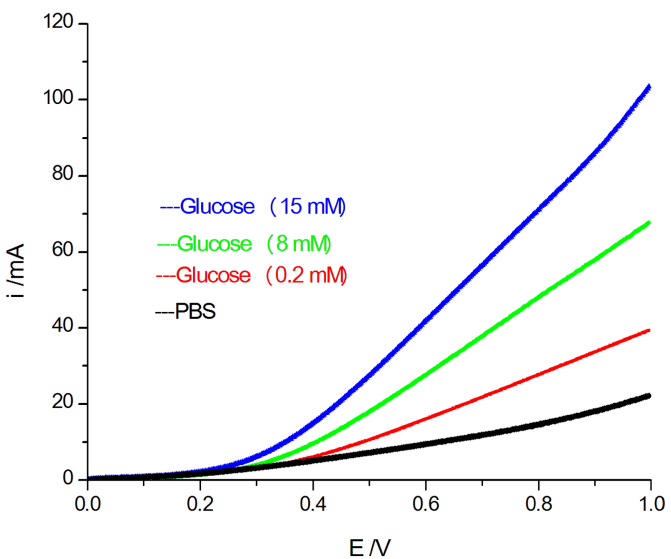
120
100
80
60
40
20
0
i /mA
---Glucose (15 mM)
---Glucose (8 mM)
---Glucose (0.2 mM)
---PBS
0.0
0.2
0.4
0.6
0.8
1.0
E /V

Figure 4

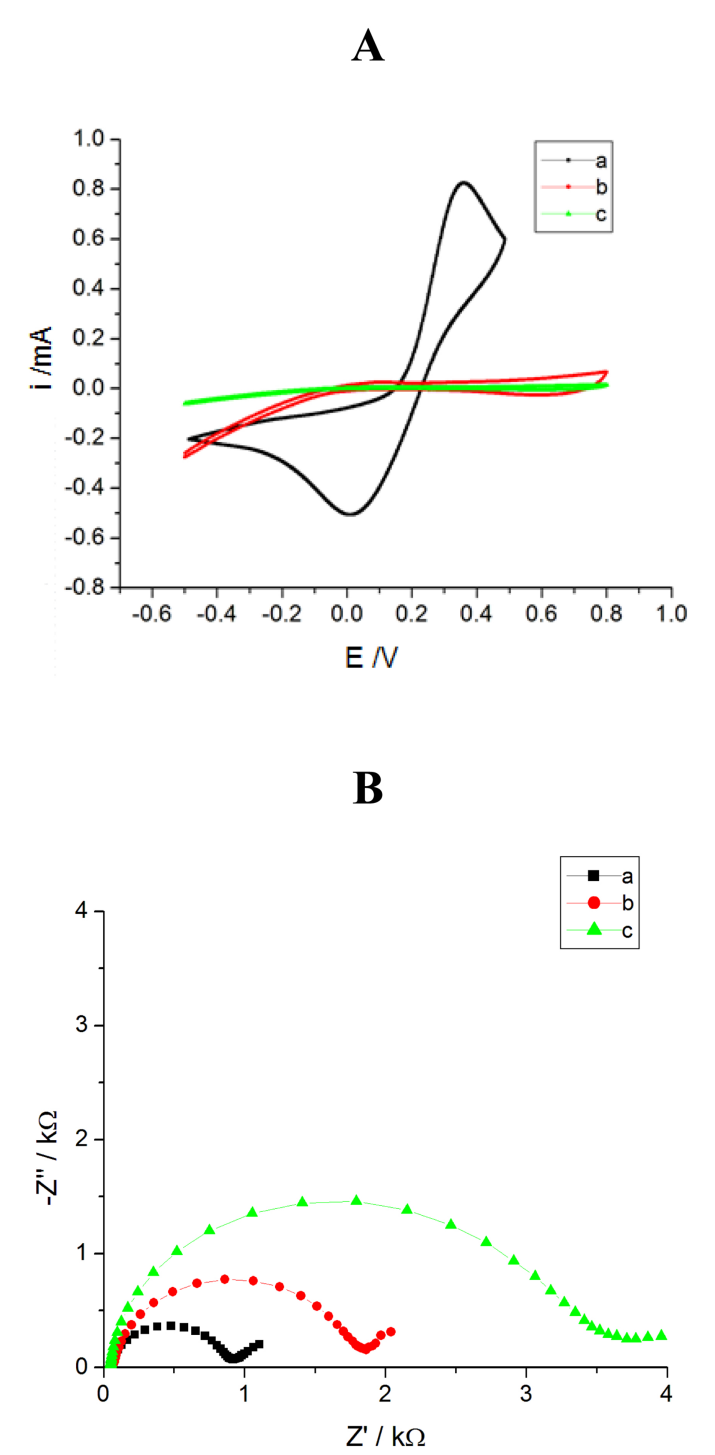
A
1.0
0.8
0.6
0.4
0.2
0.0
-0.2
-0.4
-0.6
-0.8
i /mA
-0.6
-0.4
-0.2
0.0
0.2
0.4
0.6
0.8
1.0
E /V
a
b
c
B
4
3
2
1
0
-Z'' / kΩ
0
1
2
3
4
Z' / kΩ
a
b
c

Figure 5

A

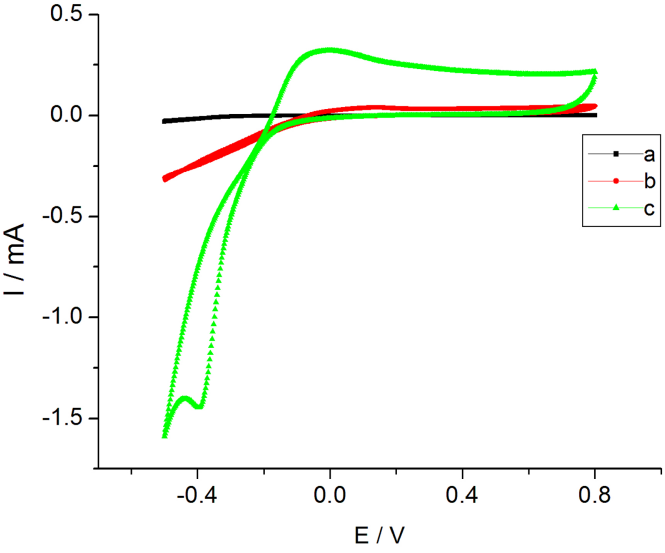

B

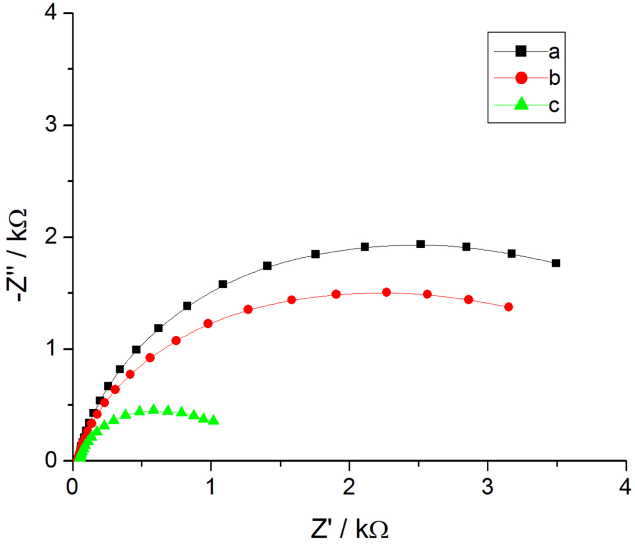

Figure 6

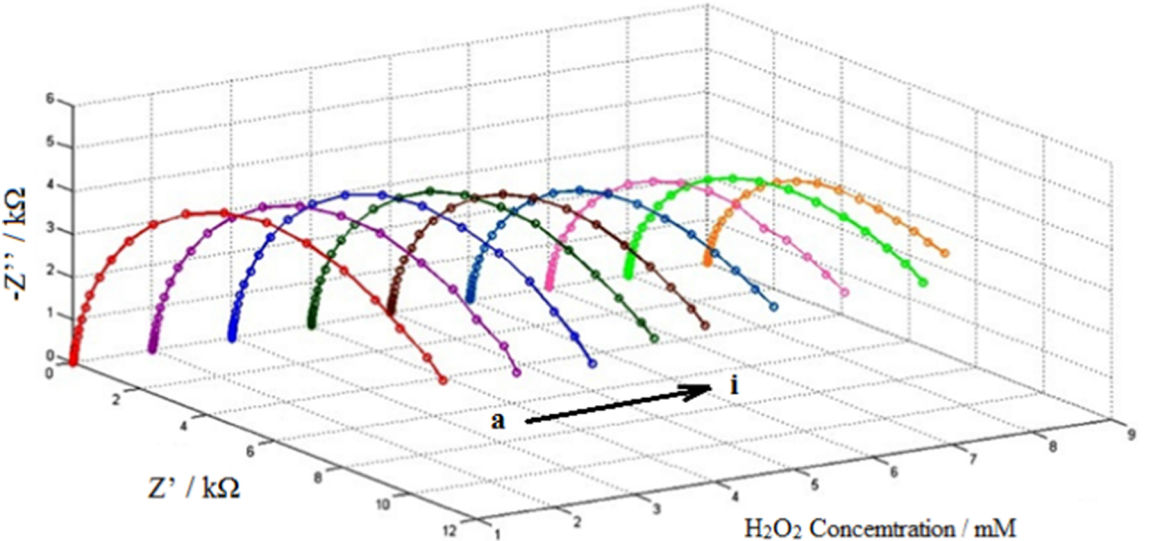

Figure 7

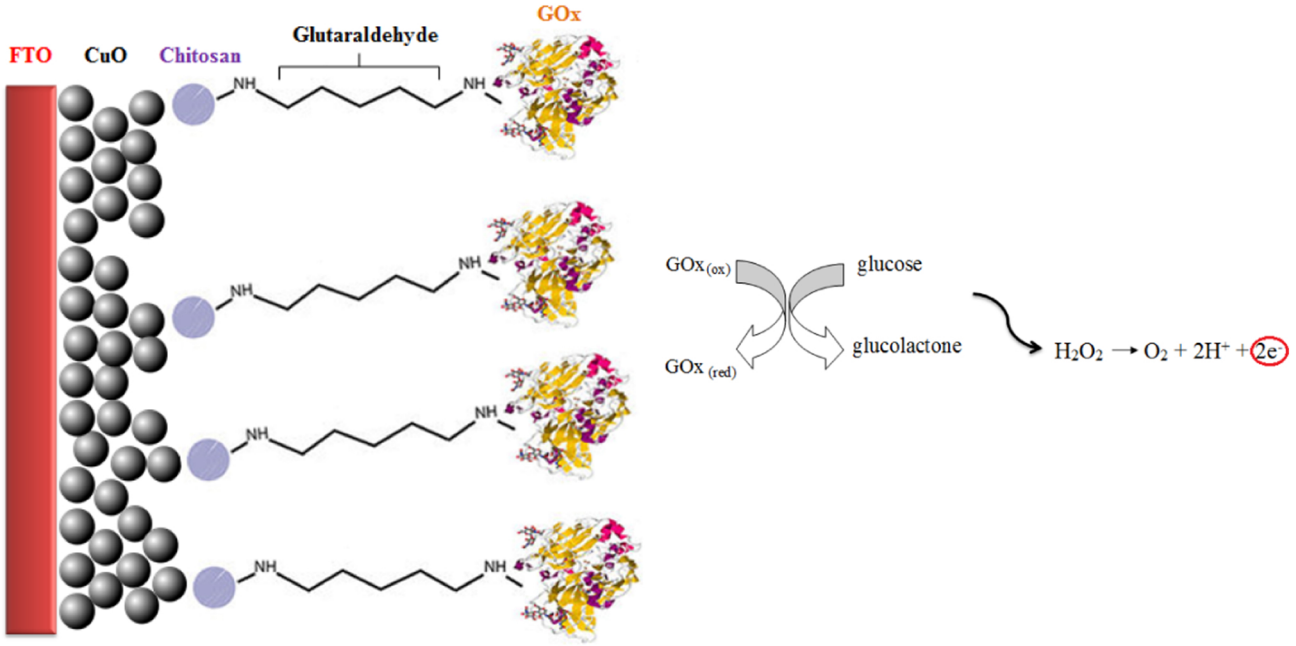
FTO
CuO
Chitosan
Glutaraldehyde
GOx
NH
NH
GOx(ox)
glucose
GOx (red)
glucolactone
H2O2 → O2 + 2H+ + 2e-

Figure 8

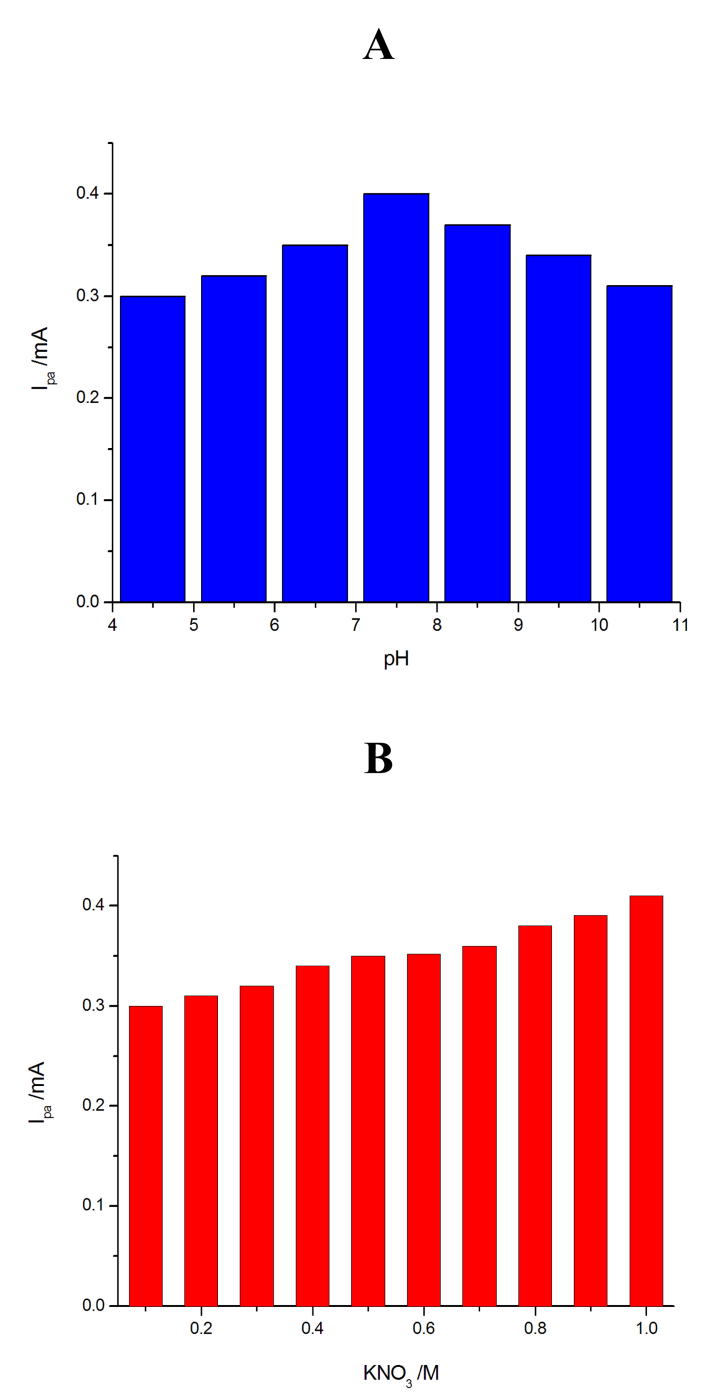
A
0.4
0.3
0.2
0.1
0.0
I_{pa} /mA
4
5
6
7
8
9
10
11
pH
B
0.4
0.3
0.2
0.1
0.0
I_{pa} /mA
0.2
0.4
0.6
0.8
1.0
KNO_3 /M

Figure 9

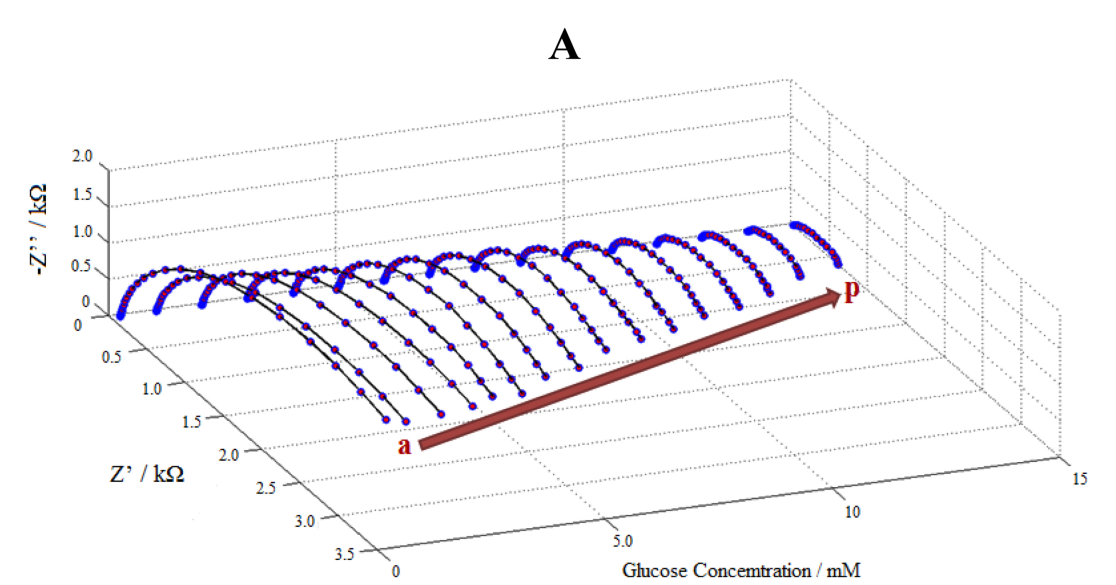
A
-Z'' / kΩ
2.0
1.5
1.0
0.5
0
0
0.5
1.0
1.5
2.0
2.5
3.0
3.5
Z' / kΩ
a
p
0
5.0
10
15
Glucose Concemtration / mM

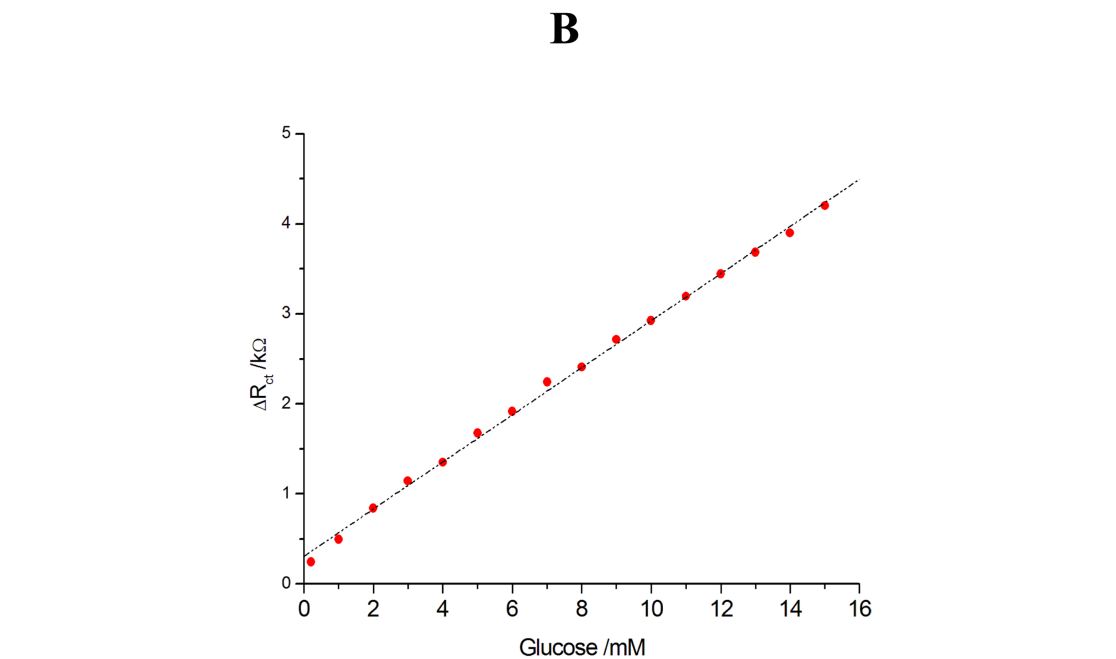
B
ΔR_ct /kΩ
5
4
3
2
1
0
0
2
4
6
8
10
12
14
16
Glucose /mM

Figure 10

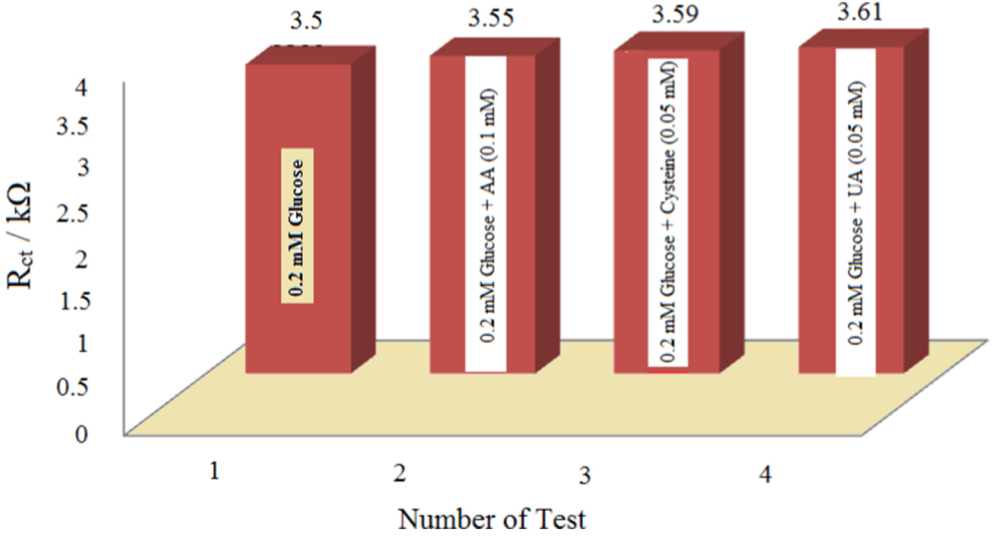
3.5
3.55
3.59
3.61
0.2 mM Glucose
0.2 mM Glucose + AA (0.1 mM)
0.2 mM Glucose + Cysteine (0.05 mM)
0.2 mM Glucose + UA (0.05 mM)
R_{ct} / kΩ
0
0.5
1
1.5
2
2.5
3
3.5
4
1
2
3
4
Number of Test

Figure 11

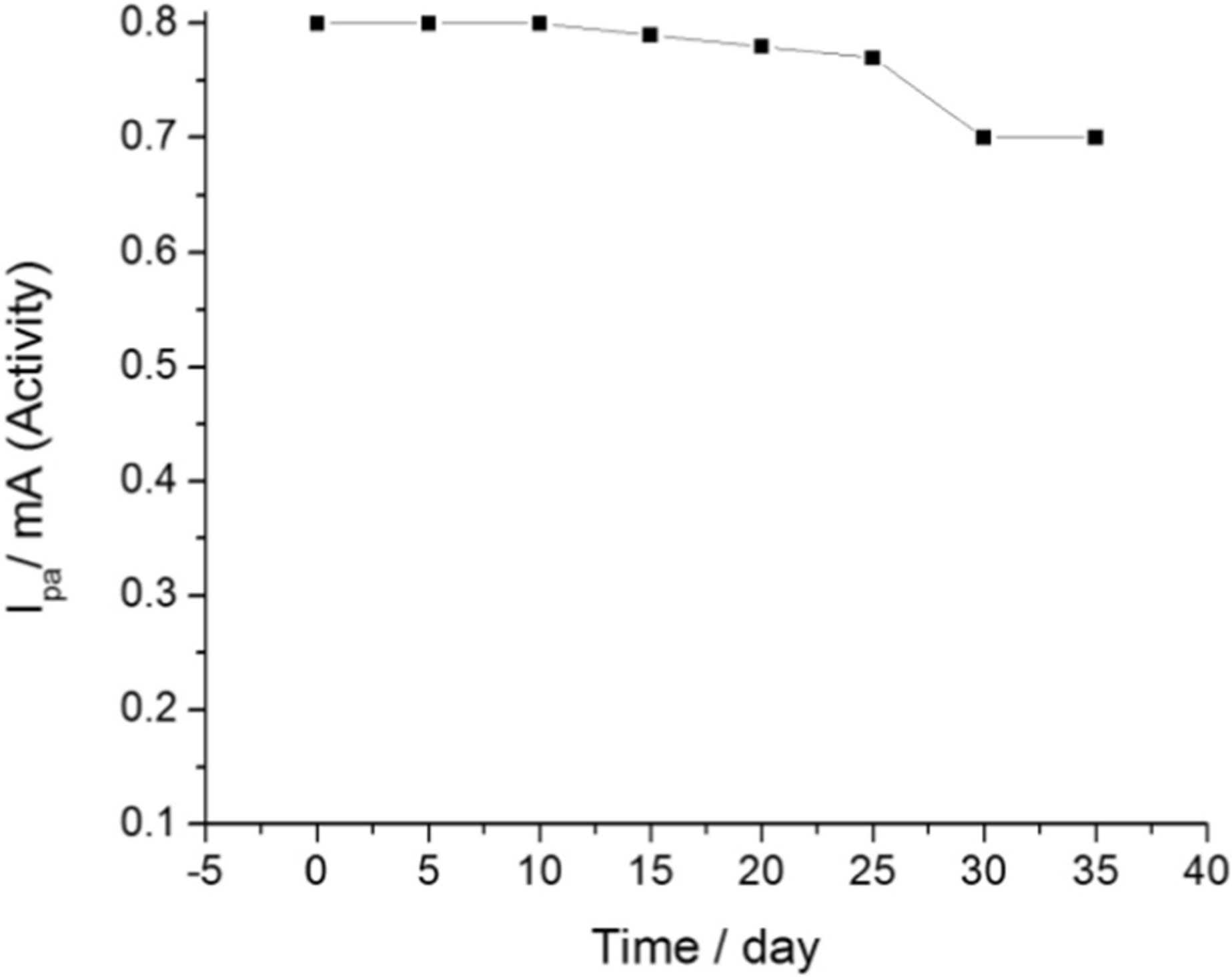
0.8
0.7
0.6
0.5
0.4
0.3
0.2
0.1
I_{pa} / mA (Activity)
-5
0
5
10
15
20
25
30
35
40
Time / day

Figure 12